

Figure 2 Distribution of address discharge lags

As previously mentioned in the introduction, we adopted statistical procedures to analyze the histograms of address discharge lags. Figure 2 shows a typical histogram of address discharge time lags. We now introduce Z value in order to compare the addressing capability of each histogram. The definition of Z value is

$$Z = \frac{T_{sc} - T_{avg}}{\sigma} \quad (2)$$

$T_{sc}$  is the width of a scan pulse,  $T_{avg}$  is the average value and  $\sigma$  is the standard deviation of a histogram, respectively. Higher Z value means better address-ability.

Figure 3 shows the result of our first experiment: the dependence of Z value on negative going Vny. It shows that address jitters are getting shorter and saturated as negative going Vny goes more negative. This phenomenon means that positive wall charges on the surface of the phosphor layer gradually diminish as Vny goes more negative. Therefore, the probability of instability due to the loss of wall charges in addressing period decreases.

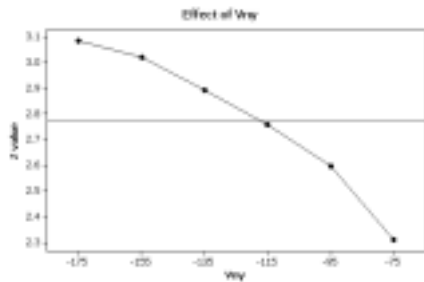


Figure 3 Dependence of Z value on Vny

2.2 Design of new ramp-reset waveforms

We obtained some information from the previous result. It was useful to reduce wall charges on the bottom of a cell for better addressability, but there was a limitation. We thought that control of wall charges on the MgO surface over the scan electrode as well as on the surface of the phosphor layer could

improve the performances further more. From the concept of simultaneous control of wall charges, we designed a new ramp-reset waveform: Dividing an erasing ramp discharge into two parts by discharge modes in time order improves addressability and reduces the black luminance.

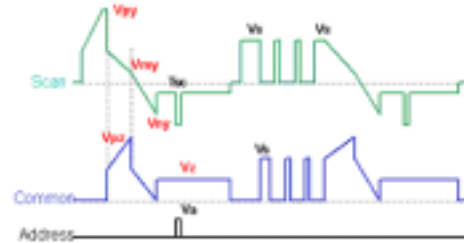
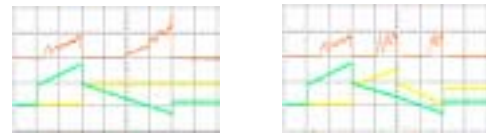


Figure 4 the DDR waveform

Figure 4 represents the DDR (Dual Discharge mode Ramp-reset) waveform. The DDR waveform has an erasing ramp period of successive surface and vertical discharges: the surface discharge between two sustain electrodes and the vertical discharge between a scan electrode and an address electrode. Figure 5 shows IR emissions from each waveform. In Figure 5(b), DDR has divided erasing ramp discharges according to discharge modes contrary to the conventional one. This divide of discharges certainly reduces the black luminance.



(a) Conventional ramp - reset (b) DDR ramp - reset

Figure 5 IR emissions of ramp-reset waveforms

However, we encountered an obstacle applying the above DDR waveform to the large size panels because of large panel capacitance of almost one hundred nano-Farads. Two ramping down phase of scan voltage cannot hold Vny when abrupt change in common electrode voltage level from Vpz to Vs occurs: capacitance coupling between scan and common electrodes is the reason. Therefore, we have to re-design DDR and Figure 6 shows this modified DDR with Vpz ramping down to zero. Nevertheless, this waveform still has a problem of requiring additional Vpz power supply.

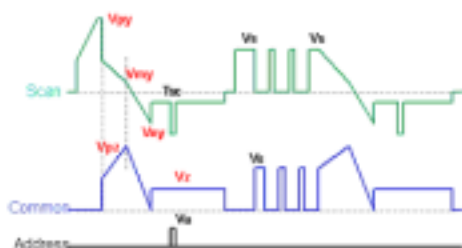


Figure 6 modified DDR

We improved DDR again eliminating the ramp up  $V_{pz}$  of waveform applied in common electrode. Figure 7 represents the simple DDR waveform. We compared the performances of three types of the DDR waveforms. Finally, we concluded that their performances have no difference in addressability and the black luminance because ramp down phase has the same effect on the panels.

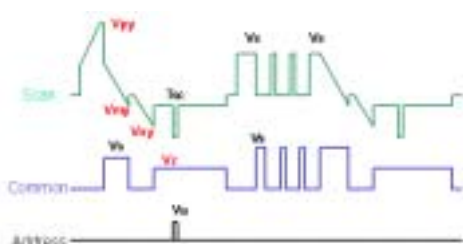


Figure 7 simple DDR

### 2.3 Result of the new ramp-reset waveform

We are now focusing on an operation of simple DDR in Figure 7. The surface discharge in the first step of erasing ramp has the similar effect with the result of Figure 3 in section 2.1. Meanwhile, the next consecutive vertical discharge could control wall charges on both sides of scan and address electrodes simultaneously.

Table I shows the result of the comparison between the conventional and DDR. We used 1.3 $\mu$ s of a scan pulse and the delay-time of 1ms prior to applying the scan pulse. The voltage level  $V_{my}$  in simple DDR is set to be -50V. In Table I, DDR shows better performances: lower black luminance of 10% as well as higher addressability of 45%.

Table I Comparison between ramp waveforms

Waveform	$V_{py}$ (V)	$V_{pz}$ (V)	Black Luminance (cd/m <sup>2</sup> )	Targ (ms)	T1 (ms)	$\delta$ (ms)	Z	%
Reference	-95	190	0.18	0.816	0.488	0.185	2.62	100%
DDR	-175	90	0.18	0.772	0.470	0.169	3.12	119%
DDR	-155	110	0.16	0.741	0.459	0.148	3.78	144%

## 3. Discussions

### 3.1 Black luminance

We have already shown IR emissions from DDR in Figure 5(b). In the conventional waveform, IR emissions from the erasing ramp period in Figure 5(a) gradually increase with time. DDR is likely to cut-off strong emissions from erasing ramp edge: the sum of IR emissions from surface and vertical discharges in DDR is weaker than that of the erasing ramp phase in the conventional waveform.

### 3.2 Fast addressing

We calculated wall charges and electric fields using the two-dimensional simulator SIPDP-AC<sup>TM</sup> [12] to support our experimental results.

Figure 8 shows distributions of charge densities after each ramp-reset waveform. DDR distributes positive wall charges more non-uniformly over the phosphor layer: wall charges on the phosphor layer below the scan electrode were erased more than those of the conventional waveform.

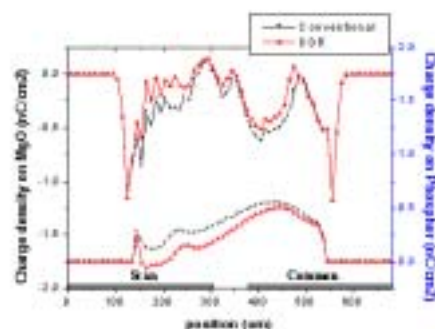


Figure 8 Charge density after ramp-reset

Figure 9 represents the electric field intensity of each waveform perpendicular to the MgO surface at an addressing moment. In DDR, the electric field intensity is greater than that of the conventional. It means that the DDR waveform has a chance to trigger a faster discharge than the conventional one.

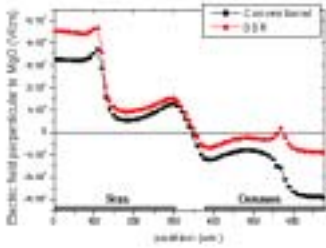


Figure 9 Electric fields at addressing period

Figure 10 shows address discharge currents at address periods. DDR shows faster addressing than the conventional expected in Figure 9.

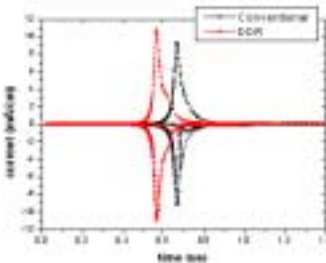


Figure 10 addressing discharge at addressing period

In the real world, address jitters do not follow exactly the simulation results because of statistical uncertainty. In general, discharge time lags have a stochastic feature and follow Laue's expression [13].

$$N / N_0 = 1 - \exp\left\{-\frac{(t - t_f)}{\tau_s}\right\} \quad (3)$$

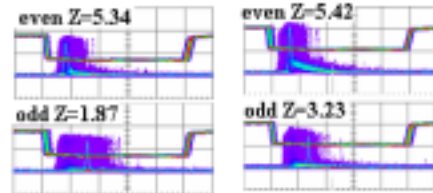
$N$  is the number of discharges after time  $t$  in  $N_0$  trials and  $t_f$  is the formative time lag. The statistical time constant,  $\tau_s$  is inversely proportional to the discharge probability,  $P_0$  and seed particle density,  $n_0$ .

$$\tau_s \propto 1 / P_0 n_0 \quad (4)$$

The discharge probability  $P_0$  is dependent on the potential distribution as well as materials and gas properties. The formative time is also dependent on potential distribution. In Table I in section 2.3, DDR affects both the formative time lag and the standard deviation. Therefore, we concluded that DDR is likely to generate more seed particles as well as to control the potential distribution on the phosphor layer. More priming particles seem to affect align-robust addressing of DDR in following section.

### 3.3 Align-robust addressing

As mentioned in previous section, DDR can reduce misalign effects of bad manufacturing better than the conventional waveform. Figure 11 shows that DDR compensate misalign effects greatly. In this case, the panel has been misaligned several tens of microns.



(a) Conventional (b) DDR

Figure 11 misalign effects of a cell; DDR reduces misalign effect greatly.

### 4. Conclusions

We investigated the relations between address discharge jitters and the ramp-reset conditions. We found wall charges on the surface of a phosphor layer dominate addressability and saturation of jitters is the limitation in the conventional waveform. We proposed new ramp-reset waveforms as well as a statistical method to analyze performances of them. New ramp-reset waveforms are fast addressable and align-robust so that they realize a single scan driving at higher resolution PDPs.

### 5. References

- [1] T.Shinoda, US Patent 5541618
- [2] L.F.Weber, US Patent 5745086
- [3] T.Kurata et al., US Patent 6294875
- [4] V.P.Nagorny et al., *J.Appl.Phys.* **77**, p3645 (1995)
- [5] V.P.Nargrny and L.F.Weber, *SID 00 digest*, p114 (2000)
- [6] K.Sakita et al., *SID 01 digest*, p1022 (2001)
- [7] H.Kim et al., *SID 01 digest*, p1029 (2001)
- [8] K.Sakita et al., *SID 02 digest*, p948 (2002)
- [9] S.T.de Zwart et al, *IDW 01*, p845 (2001)
- [10] H.Inoue et al., *Eurodisplay 2002*, p931 (2002)
- [11] M.Makino et al., *IDW 01*, p809 (2001)
- [12] [www.siglo-kinema.com](http://www.siglo-kinema.com)
- [13] M.Von Laue, *Ann.Phys.,Lpz*, **76**, p261, 1925